Journal of Coastal Research	14	4	1363–1372	Royal Palm Beach, Florida	Fall 1998

Mudbanks of the Southwest Coast of India. VI: Suspended Sediment Profiles

Yigong Li†‡ and Trimbak M. Parchure

† Coastal and Oceanographic Engineering Department
University of Florida
Gainesville, FL 32611, U.S.A.

Hydraulics Laboratory
Waterways Experiment Station
Vicksburg, MS 39180, U.S.A.

ABSTRACT

LI, Y. and PARCHURE, T.M., 1998. Mudbanks of the Southwest Coast of India. VI: Suspended Sediment Profiles. *Journal of Coastal Research*, 14(4), 1363–1372. Royal Palm Beach (Florida), ISSN 0749-0208.

Physical factors influencing suspended fine sediment loads in the region of mudbanks off Alleppey on the southwest coast of India are examined. Sediment dynamics of mudbanks is known to be predominantly governed by waves, and suspended sediment concentration in this area is closely correlated to local entrainment and settling fluxes due to waves, which at times are modulated by effects of weak currents. A simple, semi-empirical model that accounts for the vertical fluxes of fine, cohesive sediment in water and across the water-fluid mud interface due to waves and a weak current has been formulated to simulate suspension concentration profiles. The model is initially tested against laboratory flume data on wave-induced entrainment of muds, which shows the importance of mud rheology in governing resuspension. The model is then used to simulate suspended sediment concentration profiles measured near the Alleppey Pier under monsoonal waves that create mudbanks close to shoreline. Profiles are generated to represent five documented stages of mudbank evolution from formation to dissipation. Because the field data are very sparse in terms of spatial and temporal coverage, only a limited comparison of model and field is achieved. In spite of this limitation, the exercise shows that it should be possible to obtain reasonably reliable site-specific results on predicted profiles of suspended sediment over mudbanks, provided adequate field data are available for selecting representative values of the empirical parameters for calibration of the model.

ADDITIONAL INDEX WORDS: *Cohesive sediment, Fluid mud, Kerala, lutocline, monsoon, rheology, sediment entrainment, sediment resuspension, sediment settling, wave damping, wave-mud interaction.*

INTRODUCTION

The generation of turbidity by waves and currents near coastlines dominated by cohesive mud is a problem of considerable interest due to its inherent engineering and environmental implications. In Kerala State bordering the southwestern coast of India, the livelihood of local fishermen depends to a great extent on seafood catch in areas where underwater mudbanks occur (NAIR, 1988). As described by MATHEW *et al.* (1995), these mudbanks appear near sandy shores at about the time of onset of the southeastern monsoon in May/June when wave activity increases, and eventually dissipate as wave action tapers off toward the end of rainy season in August/September. Within this period, the mudbanks go through several changes with respect to their shapes and volumes, spreading rate and water column turbidity. When the mudbank is fully formed, its landward edge is typically very close to shoreline in wading water depth. In plan form the mudbank very approximately resembles a semi-elliptical disk, with its axis along the shore (Figure 1). Despite the convergence of waves toward the mudbank due to refraction, high absorption of wave energy by mud tends to minimize wave breaking in the mudbank area, even as waves break vigorously elsewhere in the surf zone along the sandy coast. The typical alongshore length of mudbank is 2 ~ 5 km, shore-normal distance is 1.5 ~ 4.0 km, and mud thickness is 1 ~ 2 m, with sediment consisting mainly of highly cohesive and flocculated clays. Each year, between the southern city of Alleppey in the State of Kerala to the northern city of Mangalore in the State of Karnataka, a distance of about 400 km, fifteen to twenty mudbanks usually occur at about the same nearshore sites during the monsoon.

MATHEW *et al.* (1995) have noted that mudbank dynamics, *i.e.*, formation, growth, transport and dissipation of mudbanks, is mainly governed by the wave field and the comparatively weak currents that occur in the area. These investigators have obtained synoptic wave measurements off Alleppey, where some suspended sediment concentration profiles were also measured under fair weather and monsoonal wave conditions (MATTHEW and BABA, 1995). Based on measurements of mud viscosity at different shearing rates as well as the upper Bingham yield strength, FAAS (1995) argued that the characteristic variations in suspended sediment concentration with seasonal progression of monsoonal waves and bottom conditions correlates with the rheological response of bottom mud to wave forcing. JIANG and MEHTA (1995) showed that the rheology of bottom mud from the area can be described by

97017 received and accepted in revision 18 January 1997.
‡ Present address: Moffatt & Nichol Engineers, Long Beach, CA 90807, U.S.A.

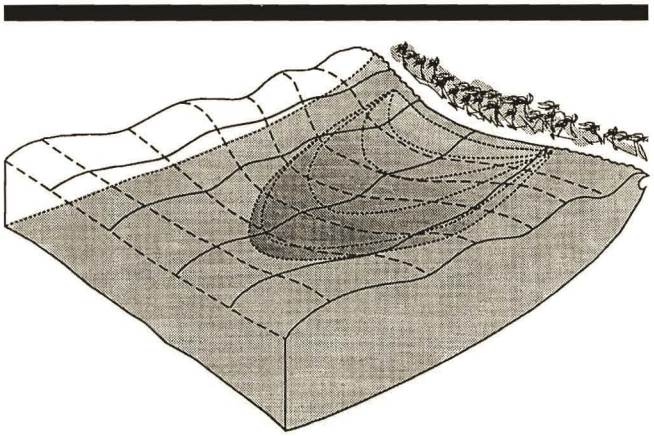

Figure 1. Schematic of a typical monsoonal mudbank along the southwest coast of India.

a viscoelastic model, which is a generalization of the Voigt model for mud proposed by, among others, MAA (1986). The viscosity and shear moduli required for the generalized model were obtained from tests in a controlled-stress rheometer. JIANG (1993) and JIANG and MEHTA (1996) further showed that these parameters can be used to calculate the characteristically high damping of monsoonal waves with a good degree of accuracy.

The problem dealt with in this paper is that connected with understanding the basic mechanism of turbidity generation in the mudbank area. This problem in its entirety is complicated by the transitory nature of the mudbanks, changes in the wave-current field and associated temporal and spatial variabilities in suspended sediment concentration. Notwithstanding these complexities, the simplified problem concerns the simulation of concentration profiles due to wave- and current-induced forcing over bottom mud. To accomplish this task a simple, semi-empirical modeling approach is used incorporating vertical fluxes of sediment in the water column and across the interface between soft bottom mud and water. Forcing by waves is considered in the presence of a current that is assumed to be so weak that it modulates the vertical turbulent mass diffusivity, without however measurably influencing the wave-determined velocity profile, or wave-induced bottom scour. This approximation enables simulation of the characteristically observed enhancement of upward diffusion of sediment derived from the bottom, without adding complexities that arise due to the inclusion of a steady or quasi-steady current field superimposed on waves. The model is first tested against laboratory flume data of MAA (1986), and is then applied to the Alleppey mudbank measurements of MATHEW (1992).

PROBLEM FORMULATION

Within a water column of depth h, vertical sediment transport is governed by upward mass diffusion due to turbulence and particulate settling. Since the time-scales of these processes relevant to turbidity generation are considerably larger than the wave period, it is permissible to examine the problem on a wave-average basis. Using C to denote wave-averaged suspended sediment concentration (or the dry density), w_s the sediment settling velocity and K_z the sediment diffusion coefficient in the vertical direction, the change in C with time at any elevation, z, (measured positively upward from the mean or still water level) is determined by the magnitude and direction of the net sediment flux due to diffusion and settling. Thus, the vertical suspended sediment transport equation can be expressed as:

$$\frac{\partial C}{\partial t} = \frac{\partial}{\partial z}\left(w_s C + K_z \frac{\partial C}{\partial z}\right) \tag{1}$$

Equation 1 can be solved for any initial condition, C(z,0), and surface (z = 0) and bottom boundary (z = −h) conditions, provided w_s and K_z are specified.

When the sediment is cohesive, w_s depends on C in a highly nonlinear way (VAN LEUSSEN, 1994). For a given sediment and water chemistry, this dependence can be expressed as (MEHTA, 1994):

$$w_s = \begin{cases} \dfrac{\alpha_1 C^{*\beta_1}}{(C^{*2} + \gamma_1^2)^{\delta_1}} = w_{sf} & C < C^* \\ \dfrac{\alpha_1 C^{\beta_1}}{(C^2 + \gamma_1^2)^{\delta_1}} & C \geq C^* \end{cases} \tag{2}$$

in which coefficients α_1, β_1, γ_1 and δ_1 depend on the rate of flow shear, and are therefore specific to the flow field being considered (WOLANSKI et al., 1992). The concentration, C*, defines the limit below which w_s (= w_{sf}) remains practically independent of C due to the very low frequency of inter-particle collisions required to promote floc growth. At concentrations above C*, w_s at first increases with increasing C due to enhanced flocculation, then decreases as settling is eventually hindered by the excessive amount of sediment in suspension. Thus, in Eq. 2 when C ≥ C*, and when $\gamma_1^2 \gg C^2$, we obtain $w_s \simeq \alpha_1 \gamma^{-2\delta_1} C^{\beta}{}_1$, which for positive values of β_1 characterizes the regime of increasing settling velocity with increasing concentration due to flocculation. On the other hand, setting $\gamma_1^2 \ll C^2$ yields $w_s \simeq \alpha_1 / C^{2\delta_1 - \beta_1}$, which for positive values of $2\delta_1 - \beta_1$ describes hindered settling.

In Eq. 1, K_z, depends on the flow field and its modulation by density stratification. Given the diffusivity under non-stratified or neutral flow conditions, K_0, we specify:

$$K_z = K_0 \phi \tag{3}$$

where ϕ is the Monin-Obukov correction for stratification, which increasingly reduces the ratio, K_z/K_0, below unity with increasing concentration gradient in the water column, or with decreasing flow energy required for entrainment (DYER, 1986). Thus, ϕ characterizes the degree of damping of neutral diffusion due to a stably stratified concentration gradient. When the wave field is modulated by a weak current, a noteworthy effect is that the eroded material is entrained upward at a measurably faster rate than when only waves are present. This effect is mainly due to the characteristically greater thickness of the current-induced boundary layer than due to waves alone. To simulate enhanced diffusion to account for the combined effect of waves and current on the vertical diffusion of suspended sediment, sophisticated models based on

wave-current boundary layer interactions have been developed (MADSEN, 1991). On the other hand, for simplicity of treatment here, we will introduce the following assumed linearized form of the neutral diffusion coefficient:

$$K_0 = \alpha_2 K_{0w} + \alpha_3 K_{0c} \tag{4}$$

in which the wave and current diffusion coefficients, K_{0w} and K_{0c}, respectively, must be specified, and also the corresponding weighting coefficients, α_2 and α_3.

For neutral diffusion under wave motion, several equations have been proposed (DYER, 1986). Focussing on the ambient water column rather than the boundary layer, and following HWANG (1989), we will select the expression proposed by HWANG and WANG (1982):

$$K_{0w} = \alpha_4 \frac{\omega \zeta_0^2}{8} \frac{\sinh^2 k(h + z)}{\sinh^2 kh} \tag{5}$$

in which $\omega = 2\pi/T$ is the angular wave frequency, T is the wave period, ζ_0 is the wave amplitude, *i.e.*, one-half wave height, k is the wave number and α_4 is a diffusion scaling coefficient, which for a given sediment depends on the flow field. Note that based on wave energy dissipation in the water column and experimental data, THIMAKORN (1984) arrived at an expression for K_{0c} that is akin to Eq. 5, with $\alpha_4 = 1.77/\sinh kh$. For diffusion due to the current-induced boundary layer the well known Prandtl-von Karman expression for K_{0c} is selected, *i.e.*,

$$K_{0c} = \frac{\kappa n g^{1/2}}{h^{1/6}} U(h - z)\left(1 - \frac{h - z}{h}\right) \tag{6}$$

where κ is Karman constant, n is Manning's bed resistance coefficient, g is the acceleration due to gravity and U is the mean current velocity. For open channel flows devoid of sediment $\kappa = 0.4$ (DYER, 1986), and this value will be used consistently, ignoring the variability in κ with suspension concentration and the flow field, in comparison with the uncertainties involved in selecting several other parameters required for concentration profile simulation. In the absence of site-specific data on bed resistance, it is acceptable to assume the bottom to be smooth, and represent its resistance by selecting Manning's $n = 0.011$ (MEHTA *et al.*, 1982). Finally, for the stratification factor, ϕ, we will select the expression of MUNK and ANDERSON (1948), which has been used by, among others, HWANG (1989) for simulating the influence of stratification under wave motion, and by ROSS (1988) for sediment-induced stratification under a tidal current. This expression is:

$$\phi = (1 + \alpha_5 Ri)^{\beta_2} \tag{7}$$

where coefficients α_5 and β_2 depend on the effect of suspended sediment on the turbulent mixing length. The gradient Richardson Number, Ri(z), which embodies the influence of stratification on the turbulent mixing energy, is defined as

$$Ri = -\frac{\frac{g}{\rho}\frac{d\rho}{dz}}{\left(\frac{du}{dz}\right)^2} \tag{8}$$

where ρ is the fluid density and u(z) is the horizontal velocity. A restriction on the application of Eq. 7 is that it is not always valid when the velocity gradient du/dz is zero, because in that case $Ri \rightarrow \infty$ by virtue of Eq. 8. Noting that u is the turbulence-mean velocity, if for example $du/dz = 0$ at some elevation where u(z) exhibits an inflexion, Eq. 3 will set diffusion to zero because $\phi = 0$, when in fact turbulent eddies may be quite effective in transporting sediment upward across that elevation. A commonly adopted, simplified approach to obviate this problem is by considering a depth-mean value of the velocity gradient over a certain characteristic wave boundary layer thickness.

To solve Eq. 1, the boundary condition at the water surface is that the net flux of sediment at $z = 0$ is nil, *i.e.*,

$$w_s C|_{z=0} + K_z \left.\frac{\partial C}{\partial z}\right|_{z=0} = 0 \tag{9a}$$

and at the water-fluid mud interface ($z = -h$) the net flux of sediment is determined by sediment entrainment, E, and deposition, S, *i.e.*,

$$w_s C|_{z=-h} + K_z \left.\frac{\partial C}{\partial z}\right|_{z=-h} = E - S \tag{9b}$$

Specification of the fluxes, E and S, is crucial to an accurate simulation of the suspended sediment profile (MEHTA, 1991a).

Sediment entrainment due to hydrodynamic instabilities at the soft mud-water interface resulting in the generation and breakup of interfacial billows by shear flows has been described in terms of the balance between production of turbulent kinetic energy, buoyancy work in entraining the sediment and viscous energy dissipation (KRANENBURG, 1994; SCARLATOS and MEHTA, 1993; WINTERWERP *et al.*, 1993; MEHTA and SRINIVAS, 1993). This process is distinct from surface erosion of sediment flocs, which occurs over typically harder cohesive beds (TAKI, 1990; PARCHURE and MEHTA, 1985). Bottom hardness depends on mud density and the dynamic state of mud. Under continued wave action, mud can be liquefied by the cohesive bond loosening effects of cyclic normal and tangential stresses (MEHTA *et al.*, 1995; DE WITT, 1995; SANFORD, 1994). The resulting fluidized bottom is prone to destabilization and entrainment in bulk. Thus, for instance, in Lake Okeechobee in south–central Florida, comparatively dense bottom mud remains fluidized indefinitely by wind generated waves (KIRBY *et al.*, 1994).

The entrainment flux, *i.e.*, dry sediment mass entrained per unit bottom area per unit time, of fluid-like mud under wave motion can be expressed as (LI, 1996):

$$E = \begin{cases} \alpha_6 \rho_m u_b \left(\dfrac{Ri_{gc}^2}{Ri_g} - Ri_g\right) & Ri_g < Ri_{gc} \\ 0 & Ri_g \geq Ri_{gc} \end{cases} \tag{10}$$

where, for a given sediment the empirical coefficient, α_6, depends mainly on the flow field, u_b is the wave-induced horizontal velocity amplitude just outside the bottom wave boundary layer and ρ_m is mud density. Note that when using theory to determine u_b, for practical purposes it can be eval-

uated at z = −h. The global Richardson Number for wave motion is expressed as:

$$\mathrm{Ri}_g = \frac{\delta g \dfrac{\Delta\rho}{\rho_m}}{(\Delta u)^2} \tag{11}$$

where $\delta = (2\pi\nu/\omega)^{0.5}$ is the viscous wave boundary layer thickness used as a scaling parameter, ν is the kinematic viscosity of water, $\Delta\rho = \rho_m - \rho$ is the water-mud interfacial density jump and Δu is the absolute value of the maximum difference between wave velocities across the interface. In Eq. 10, Ri_{gc} is the critical value of Ri_g above which there can be no entrainment (other than that at the molecular scale), due to the strong stabilizing effect of the bottom fluid mud, or due to weak wave motion.

By virtue of the definition of Ri_g, the rate of entrainment depends on the properties of bottom mud. Thus, in addition to the effect of mud density, ρ_m, E varies with Δu, which in turn also depends on ρ_m, on mud thickness h_m, and on the rheological properties of mud (JIANG and MEHTA, 1992). In laboratory flume tests MAA (1986) observed that under certain conditions specified by the wave field and mud properties, Δu was measurably larger than the near-bottom velocity, u_b, due to the out-of-phase motion of bottom mud relative to water just above the interface.

LI (1996) conducted wave flume experiments on the resuspension of mud from the Chang Jiang River estuary in China, and also reanalyzed results from similar experiments of MAA (1986) summarized by MAA and MEHTA (1987), that were conducted with mud from an estuary near Cedar Key in Florida. In both groups of experiments waves caused the surficial layer of bottom mud to become fluid-like, then entrain and diffuse upward. Wave height, period and suspended sediment profiles were measured at different times and positions. Also reported were mud density and the settling velocity characteristics of the suspended material. From each sets of test runs, concentration profiles that ultimately developed at equilibrium were used to calculate E. Note that because E is equal to S at equilibrium the equalities, $E = S = w_s \bar{C}$, hold. Thus, E can be obtained indirectly from S, which must be determined from measurements close to the mud-water interface. However, from the concentration profile data of smLi (1996) it was found that depth-average concentrations calculated from these profiles were more reliable in terms of experimental accuracy than concentrations near the bottom. Therefore, following KRONE (1993), $\bar{C}$ is considered to be the depth-averaged concentration, characteristically equal to the concentration of a uniform, mixed-layer of suspension above bottom. The requisite settling velocity, w_s, was obtained from Eq. 2 using $\bar{C}$ and sediment-specific values of the associated coefficients. In this context it should be pointed out that from experiments on wave-induced resuspension of cohesive beds, THIMAKORN (1984) and CERVANTES *et al.* (1995) showed that the near-bottom settling flux bears a proportional relationship with the corresponding depth-average flux, and in their tests this constant at equilibrium was close to unity. From this observation one can infer that the concentration profiles in those tests were fairly uniform at equilibrium.

To determine the values of Ri_g the velocity difference, Δu, in Eq. 11 was calculated by using first order solutions of a second order analytic model developed by JIANG (1993) and summarized by JIANG and MEHTA (1996), to simulate wave damping over Alleppey mudbanks. In this approach, water is treated as a viscid fluid that is free of sediment. The rheometry required for this application has been prescribed by JIANG and MEHTA (1995) for determining mud viscosities and shear moduli of elasticity. Note that to simplify the method of analysis for determining the entrainment rate function, u_b in Eq. 10 was calculated from the analytic model by considering the bottom mud to have an arbitrarily high value of the shear modulus. The same model was used to determine the horizontal velocity gradient, du/dz, in terms of the mean value of this gradient over the wave-boundary layer, for calculating the Richardson Number, Ri, in Eq. 8.

The plot of the dimensionless entrainment flux, $E/\rho_m u_b$, versus Ri_g with data points derived from the above analysis is shown in Figure 2, in which Eq. 10 has also been plotted, with the best-fit value of $\alpha_6 = 2\times10^{-6}$. Through a separate analysis of the data of LI (1996) comprising of near-bottom concentration measurements and visual observations of the interface, it was found that the critical global Richardson Number, Ri_{gc}, was independent of the characteristic interfacial Reynolds Number, $\mathrm{Re}_\Delta = \delta\Delta u/\nu$, in the range of 100 to 350. Within this range, the mean value of Ri_g was found to be 0.043. This value is also applied to the data of MAA (1986), since from that study an independent estimate of Ri_{gc} could not be made. Notwithstanding the evident paucity of data points as well as clustering and smear, the trend of Eq. 10 in Figure 2 is seen to be in general agreement with the data points, and is analogous to the trend found for entrainment of fluid-like mud under steady shear flows (MEHTA and SRINIVAS, 1993). In consonance with the mechanics of entrainment of a salt water layer into fresh water it is seen that at low values of Ri_g, E varies with Ri_g^{-1}, which in turn can be shown to mean that the rate of entrainment is proportional to the rate of change of potential energy of the suspension. As Ri_g increases, it becomes increasingly difficult for the flow to lift sediment, with the result that E decreases rapidly when Ri_g exceeds about 0.03, and a total cutoff of entrainment occurs at $\mathrm{Ri}_g = 0.043$, assuming molecular diffusion to be negligible.

It must be pointed out the application of Eq. 10 to field data may not be straightforward, because of the scaling effects represented by the Reynolds Number, Re_w, which can be higher in the field than in flume experiments. Nevertheless, note that defining $\mathrm{Re}_w = a_b^2\omega/\nu$ (MAA and MEHTA, 1987), where $a_b = u_b/\omega$ is the near-bottom amplitude of wave-induced horizontal excursion, the ranges of Re_w in the experiments of MAA (1986) and LI (1996) were approximately 3.1×10^3 to 7.8×10^3 and 1.3×10^5 to 1.0×10^6, respectively. Therefore, the overall range of Re_w represented in Figure 2 is fairly wide, encompassing incipient turbulent to fully turbulent flow characteristic of field conditions. In turn, the observation that the two sets of data are affine, when plotted in terms of the dimensionless groups in Figure 2, suggests that scaling may have been at least partly accounted for in Eq. 10. In any event, it is necessary that the main scaling

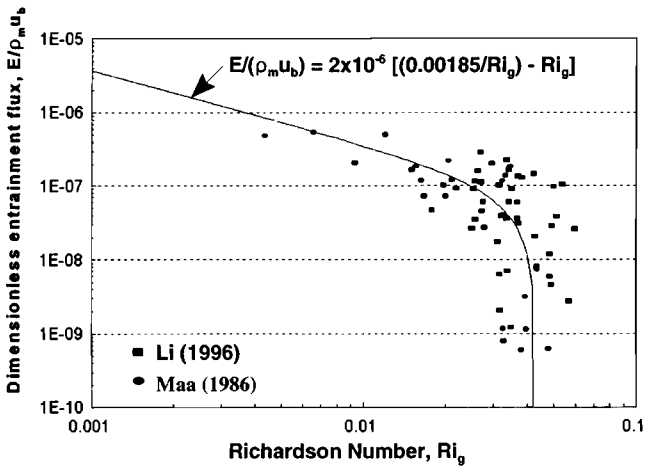

Figure 2. Dimensionless entrainment flux as a function of Richardson Number.

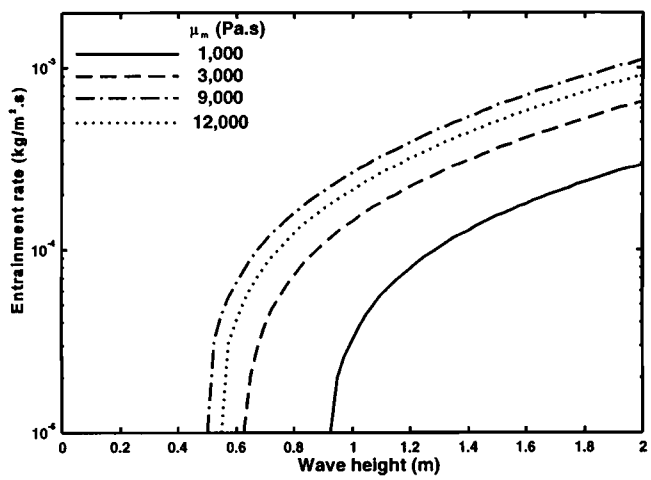

Figure 3. Entrainment flux as a function of wave height and mud viscosity.

parameter, α_6, be determined by calibration for each site-specific case.

Concerning $\alpha_6 = 2\times10^{-6}$ in Figure 2 note that the results of MAA (1986) were obtained by assuming ρ_m to be the depth-averaged value, even though mud density increased somewhat with depth in his experiments. On the other hand, bottom mud in LI's (1996) experiments was specially prepared to entail fairly uniform densities. Thus, the general agreement between data trends in the two sets of experiments suggests that in Figure 2 the effect of a non-uniform density profile on the entrainment flux has been masked in an unquantifiable way. A reanalysis of MAA's (1986) data to account for bottom density variation with depth could reveal this effect in principle; however, the density data were not accurate enough near the interface to enable such a reanalysis.

The sensitivity of E to Δu is illustrated in Figure 3 in terms of the dependence of E on wave height, $2\zeta_0$, and mud viscosity, μ_m. For each height and viscosity, E was calculated by using the following parameters applicable to a "typical" condition at Alleppey: water depth h = 3.0 m, mud thickness h_m = 2.0 m, wave period T = 8.5 s, mud density ρ_m = 1,270 kg/m^3, entrainment coefficient $\alpha_4 = 2\times10^{-5}$ and mud shear modulus G = 2,000 Pa. In Figure 3, observe the dependence of the entrainment flux on wave height. Thus, for example, selecting a characteristic value of the viscosity, μ_m, equal to 9,000 Pa.s, there will be practically very little turbidity when waves are lower than about 0.5 m. On the other hand, as the height increases above about 0.5 m, entrainment is observed to increase logarithmically in qualitative agreement with typical episodic increases in nearshore turbidity due to severe waves. The influence of viscosity at a given wave height is seen to be non-monotonic. Thus, as μ_m increases entrainment increases at first because Δu increases. However, as μ_m increases from 9,000 to 12,000 Pa.s the entrainment flux decreases because mud becomes less responsive to wave motion than at 9,000 Pa.s. FAAS (1995) has examined the behavior of Alleppey mud in terms of the stress versus rate of strain relationship to make essentially the same point, *i.e.*, the non-monotonic response of bottom mud relative to turbidity generation over the mudbanks.

The deposition flux in Eq. 9 can be expressed as:

$$S = pw_sC|_{z=-h} \tag{12}$$

where p is the probability of deposition of suspended sediment over the fluid-like mud surface. According to KRONE (1993), $p = (\tau_{cr}-\tau_b)/\tau_{cr}$, where τ_b is the shear stress at the interface and τ_{cr} is defined as the critical shear stress above which there can be no deposition. The critical shear stress further depends on the properties of flocs in the flow field, and has been found to depend on the size distribution of suspended sediment (MEHTA, 1988). We note that p = 0 corresponds to the condition when no deposition can occur, and p = 1 implies complete deposition of all suspended sediment. Since a restriction on the ability of sediment to deposit can only be modeled when the dependence of τ_{cr} on sediment properties is known, for the solution of many practical problems for which such information is not available it is best to set $\tau_b/\tau_{cr} = 0$, *i.e.*, p = 1. In other words, deposition is permitted under any flow condition as long as there is sediment in suspension, with the rate of deposition equal to the product of settling velocity and bottom suspension concentration in accordance with Eq. 12. Suspension concentration profile simulations using laboratory flume data as well as field data have been carried out successfully through this approach (CERVANTES *et al.*, 1995; SANFORD and HALKA, 1993).

LABORATORY SIMULATIONS

For testing Eq. 1, laboratory flume Runs 4, 5 and 6 of MAA (1986) were selected. Since subsets of the same experimental data were used in calculating the parameters for Eq. 10, this examination cannot be considered as a true means of validation of the method of simulation. On the other hand, concerning Eq. 10, the tests of LI (1996) constituted an indepen-

dent data set, so that the use of the more comprehensive data of MAA (1986) can be considered to be at least partially justified as a procedure for model testing. In MAA's (1986) experiments, Cedar Key mud was entrained by changing the wave conditions in steps so as to increase the applied bottom shear stress in steps. Starting with a water column of known residual or initial concentration distribution, C(z,t), the first (monochromatic) wave loading was maintained for 3 to 7 hours, then it was increased and continued for another 3 to 7 hours. In Run 6 a third wave loading, increased from the second one, was maintained for 4 hours. Suspended sediment samples were taken for each wave loading at variable time intervals, *e.g.*, 15, 30, 60, . . . minutes, at three selected elevations. Wave height, period and crude density profiles of bottom mud were also measured. Mud rheology was characterized by a Voigt viscoelastic solid, for which the viscosity, μ_m, and the shear modulus of elasticity, G, were determined in separate rheometric tests as functions of mud density (MAA, 1986).

Relevant parameters for settling and entrainment were derived from the study of MAA (1986) as well as from wave-induced resuspension studies of HWANG (1989) and ROSS (1988), and current-induced resuspension simulations of ROSS (1988). Accordingly, the settling velocity related parameters in Eq. 2 were selected to be: $w_{sf} = 6.37\times10^{-7}$ m/s, $C^* = 0.1$ kg/m^3, $\alpha_1 = 0.01$, $\beta_1 = 1.33$, $\gamma_1 = 1.5$ and $\delta_1 = 9$. Since no current was externally imposed in the experiments, it is appropriate to set $\alpha_1 = 1$ and $\alpha_3 = 0$ in Eq. 4. Calibrated values of the wave diffusion related parameter, α_4, in Eq. 5 given in Table 1 are seen to range from 0.19 to 0.60. These values are considerably larger than $\alpha_4 = 0.0008$ used by ROSS (1988), signifying a much greater upward diffusion in the tests of MAA (1986). For resuspension of 0.2 mm sand, HWANG and WANG (1982) found α_4 to range from 0.13 to 0.20 for non-breaking waves, which is comparable with the range in Table 1. The stratification parameter, ϕ, in Eq. 7 was characterized by $\alpha_5 = 0.5$ and $\beta_2 = 0.5$. These values are within the ranges of the two parameters used in previous studies on stratified flows. Thus, we note that from a compilation of such studies ROSS (1988) found α_5 to range from 0.062 to 180 and β_2 from -0.75 to 0.50. The entrainment coefficient, α_6, in Eq. 10 was selected to be 2.5×10^{-5} for the three runs. This value is higher than $\alpha_6 = 2\times10^{-6}$ in Fig. 2 because the latter value is inclusive of the influence of settling in the experiments of MAA (1986) and LI (1996), whereas, since in Eq. 9b deposition is treated separately from entrainment, a higher value of α_6 had to be chosen to simulate the concentration profiles. The critical global Richardson Number, Ri_g, was assumed to be 0.043, as in Figure 2. Input parameters required for simulations of Runs 4, 5 and 6, other than those already prescribed, are listed in Table 1.

Figure 4a shows the time-variation of simulated suspended sediment concentrations at three elevations in Run 4 (MAA, 1986). From the time of commencement of wave motion the concentrations are observed to have increased and practically approached equilibrium values by the end of the duration over which constant wave conditions were maintained. When wave height was increased, concentrations increased again to approach higher equilibrium values. Model results approximately mimic data trends over the entire test time range, with the possible exception of the initial part of the first phase (step) at the highest elevation (-12.4 cm), during which the model slightly under-predicted concentration. For results of Run 5 shown in Figure 4b, the simulations measurably under-predict the concentrations at the two upper elevations during the first step of the test. Since, however, during the second step the agreements are better, we are led to suggest that at the beginning of Run 5 the bottom material was considerably looser than assumed in the model. This situation probably arose because the bottom mud was stratified with respect to density, whereas for simulation, ρ_m was obtained by vertically averaging the bottom density profile. Thus, ρ_m was greater than the actual density during the initial phase of entrainment. Unfortunately, this explanation is not entirely consistent with the trends for the lowest elevation at -18.5 cm, where there seems to be an over-prediction followed by under-prediction during the first step. We suspect that experimental errors are at least partly responsible for the observed differences between data points and simulation. Finally, we note that in Run 6 (Figure 4c), in which entrainment occurred in three steps, simulated and data trends are generally in agreement, although in this case the lack of data points at the two lower elevations during the third step precludes a fuller comparison between model results and measurements.

Table 1. *Parameters for simulating wave flume Runs 4, 5 and 6 of Maa (1986).*

Run No.	4	5	6
Water depth (m)	0.264	0.194	0.274
Mud depth (m)	0.093	0.16	0.105
Mud density (kg/m^3)	1,080	1,080	1,100
Diffusion parameter, α_4	0.19	0.50	0.60
Mud viscosity (Pa.s)	15	21	64
Shear modulus (Pa)	168	102	123
Step no.	1	1	1
Period (s); Height (m)	1.6; 0.034	1.7; 0.032	1.8; 0.035
Duration (min)	0 to 285	0 to 230	0 to 180
Step no.	2	2	2
Period (s); Height (m)	1.1; 0.055	1.2; 0.052	1.4; 0.045
Duration (min)	285 to 588	230 to 537	180 to 425
Step no.			3
Period (s); Height (m)			1.0; 0.053
Duration (min)			425 to 670

ALLEPPEY MUDBANKS

According to the work of MATHEW (1992) conducted during the 1986–89 period, and later reported by MATHEW *et al.* (1995), the following characteristic wave conditions occurred off Alleppey. The significant wave height during the fair weather period from October to April was less than 0.75 m most of the time with no significant inter-annual variability. During the monsoon period from about May to September, the significant wave height reached 2 ~ 3 m maximum. The wave period ranged between 10 ~ 18 s for the fair weather period and 7 ~ 10 s in the monsoon, signifying a greater contribution to wave energy from the shorter period sea in the monsoon in contrast with the fair weather condition when

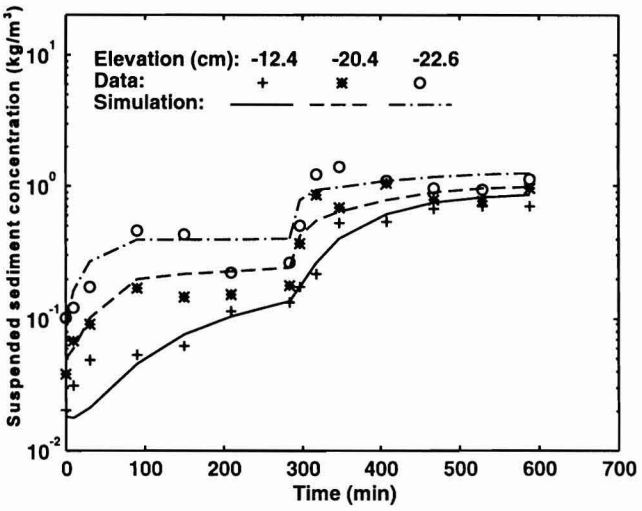

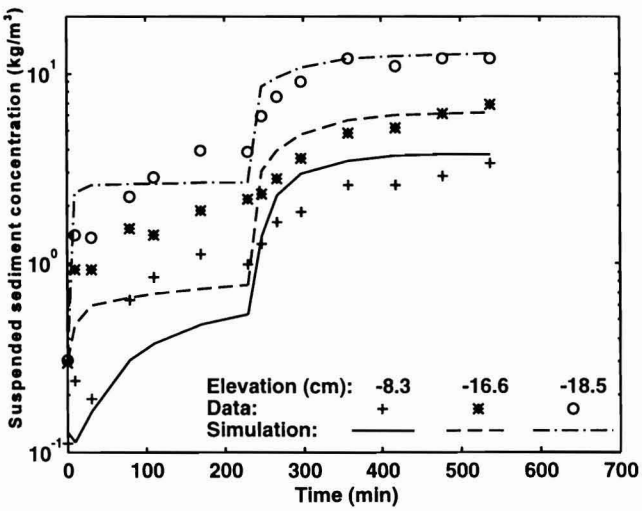

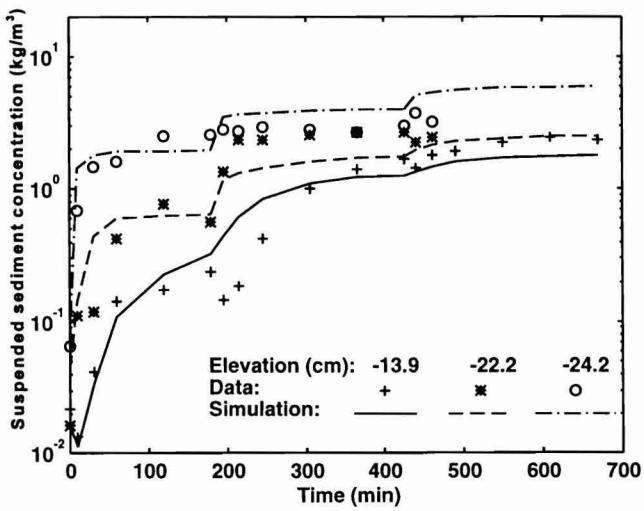

Figure 4a. Comparison between simulated and measured data for Run 4 of MAA (1986). Elevations are with reference to mean water level.

Figure 4b. Comparison between simulated and measured data for Run 5 of MAA (1986). Elevations are with reference to mean water level.

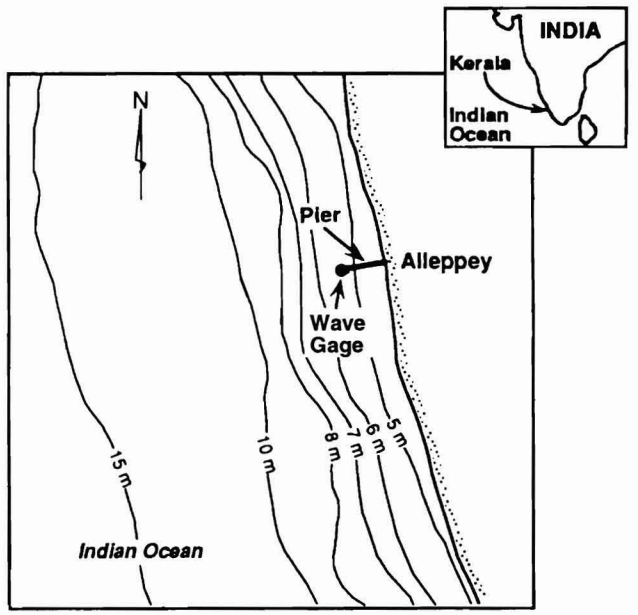

Figure 5. Region off 300 m long Alleppey pier, where suspended sediment profiles were obtained by MATHEW (1992).

wave energy was mainly imparted by the longer period swell activity. In the monsoon, most of the wave spectra were found to be single-peaked and energy was largely confined to the 0.05 ~ 0.5 Hz frequency ($\omega/2\pi$) range. The spectral peaks, which were mostly observed at 0.09 ~ 0.1 Hz (10 ~ 11 s) before the mudbank, shifted to about 0.11 ~ 0.13 Hz (8 ~ 9 s) upon formation of mudbank. Overall, 10.5 s can be chosen as a representative wave period for the pre-mudbank condition, and 8.5 s for all subsequent states of the mudbank.

A bottom-mounted pressure gage installed at the end of the Alleppey Pier (Figure 5) yielded wave information necessary to simulate the suspended sediment profiles, which were obtained by lowering suspension collectors from a boat in the same general area. As for bottom mud, it is believed that the damping of waves provides a net forward thrust which pushes mud from deeper (~ 20 m) offshore waters toward the shore (JIANG, 1993). At the same time, wave refraction effects cause this mud to accumulate where the wave energy is focussed. As a result, the thickness of fluid-like mud was about 2 m during the formation phase of the mudbank and in the period immediately after formation (MATHEW and BABA, 1995).

Characteristically, the wave height inside the mudbank area decreases once bottom mud is in place, as does turbidity, due to its correlation with wave height. Eventually, toward the end of the monsoon as the incoming energy decreases, wave-induced forward thrust is no longer sufficient to hold

←

Figure 4c. Comparison between simulated and measured data for Run 6 of MAA (1986). Elevations are with reference to mean water level.

Table 2. *Parameters for simulating Alleppey mudbank data of Mathew (1992).*

Mudbank State	Before Formation	During Formation	Full Formation	Early Dissipation	Later Dissipation
Water depth (m)	5.0	3.0	3.0	4.0	4.0
Mud depth (m)	0.05	2.00	2.00	1.00	1.00
Wave height (m)	1.23	0.77	0.31	0.50	0.45
Wave period (s)	10.5	8.5	8.5	8.5	8.5
Current velocity (m/s)	0.00	0.00	0.01	0.04	0.05
Diffusion parameter α_4	0.19	0.02	0.02	0.02	0.02

the mud against the nearshore steeper bottom slope. As a result, mud slides back toward the deeper offshore region. At Alleppey, as wave action decreases, the mudbank has been observed to begin to dissipate through shore-normal as well as lateral spreading, aided by very weak currents. At this stage its average thickness decreases to about 1 m. At the end of the monsoon, during the later stages of dissipation, wave height and turbidity drop further before offshore slide causes the mud layer to reduce to just a few centimeters in thickness (MATHEW and BABA, 1995).

For a characteristic Alleppey mud density of 1,270 kg/m^3, mud rheology was found to be best described by a Voigt-like viscoelastic solid (JIANG and MEHTA, 1995). Representative values of the viscoelastic parameters were: μ_m = 6,846 Pa.s and G = 1,965 Pa, which signifies a highly viscous material with a moderate degree of elasticity. In fair weather, suspended sediment concentrations near the surface were less than 0.007 kg/m^3, while in the lower part of the water column the concentration reached a maximum of 0.064 kg/m^3. However, with the onset of the monsoonal waves but before the mudbank was formed, the concentration in the upper portion of water column was observed to increase to 0.6 ~ 0.9 kg/m^3. Following mudbank formation a few days after the arrival of the monsoon, the concentration reduced to less than 0.1 kg/m^3 due to a decrease in wave height by damping.

For purposes of simulation, the settling velocity data and relationships shown in Figure 6 were used, based on information provided by MATHEW (1992). Also, we selected α_2 = α_3 = 1, thus assuming equally weighted neutral wave and current diffusion coefficients in Eq. 4. Selected values of α_4 characterizing wave diffusion (Eq. 5) are given in Table 2, which also lists other relevant parameters for the five characteristic phases or states of the Alleppey mudbank identified by MATHEW (1992). The water and mud depths and wave height and period are based on measurements, while the current velocity values are assumed based on qualitative observations by MATHEW (1992). Before formation of mudbank, calibrated values of the diffusion parameter, α_4, was relatively large (0.19) due to spilling breakers in the nearshore region, and became smaller (0.02) when the mudbank was formed, as wave breaking became comparatively minor due to energy absorption by mud. We note that for simulating the resuspension of mud in Lake Okeechobee in Florida, HWANG (1989) found α_4 = 0.016 as the best-fit value, which is in agreement with 0.02 selected here.

Parameters characterizing stratification, α_5 and β_2, were

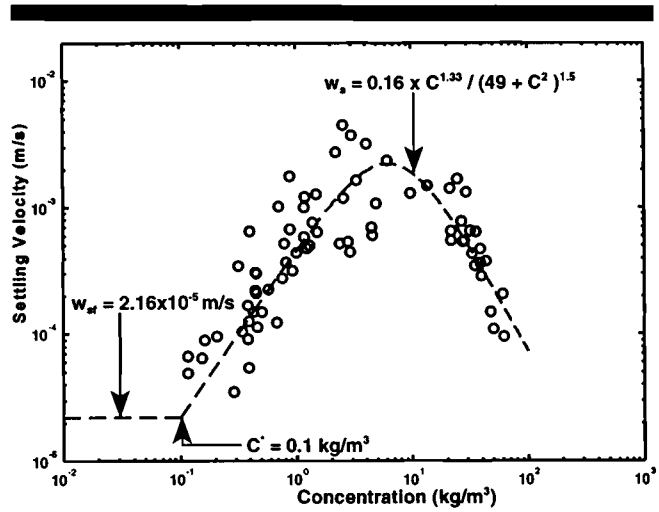

Figure 6. Settling velocity data used for mudbank turbidity simulation.

selected to be 0.5 and 0.33, which are close to those selected by HWANG (1989). For all simulations the entrainment coefficient, α_6, was chosen as 2×10^{-5}, obtained as the best value through model calibration against the measured suspension profiles, while the critical global Richardson Number Ri_g was selected to be 0.043 in the absence of specific data for Alleppey mud. The relevant range of the wave Reynolds Number, R_w, was 1.1×10^6 to 1.3×10^6, which is comparable with the upper limit of R_w in the entrainment tests of LI (1996).

As observed from simulated profiles in Figure 7a under equilibrium or near-equilibrium conditions before mudbank was formed, comparatively high wave energy and associated vertical mass diffusion led to relatively high suspended sediment concentration. This plot and other analogous ones in Figure 7 also show the formation of a significant concentration gradient near the bottom. The occurrence of such a gradient is suggested in the observations of MATHEW and BABA (1995), although their sampling was largely limited to the upper part of the water column. In that context, it is noteworthy that careful near-bottom measurements elsewhere have shown the way in which this gradient, which is qualitatively akin to the commonly observed concentration gradient called lutocline, rises and falls under wave forcing (KEMP and WELLS, 1987). Lutoclines however characteristically occur at higher concentrations, so that the simulated gradient in the present cases cannot be classified as a true lutocline. In any event, observe that during mudbank formation, the reduction in wave energy caused the concentration to decrease by an order of magnitude, and at the same time the concentration gradient came closer to the bottom (Figure 7b).

MATHEW (1992) noted that once the mudbank was fully formed, a weak alongshore current appeared; however, no measurements were reported. It is therefore interesting to note that for the simulation of suspended sediment profile for the formed mudbank condition (Figure 7c) as well as during the stages of dissipation, a small current velocity, U, ranging from 0.01 to 0.05 m/s was required for matching measured and simulated concentrations. In any event, the effect of cur-

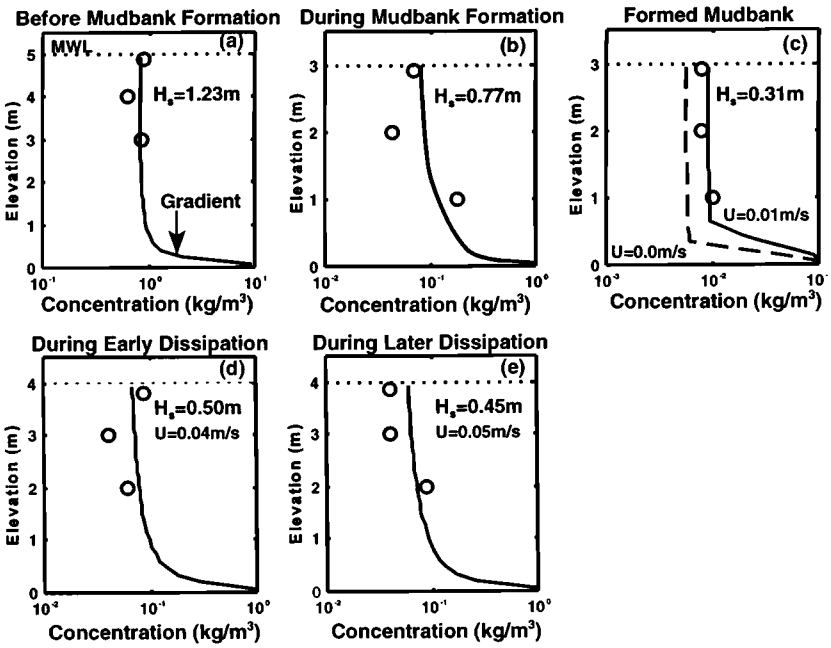

Figure 7. Simulated (continuous and dashed lines) suspended sediment concentration profiles and data (open circles) of MATHEW (1992) in the vicinity of Alleppey pier.

rent is to lift the concentration gradient due to enhance upward diffusion of the entrained material. This effect is evident in Figure 7c, in which the profile without current (dashed line) is observed to shift to the profile with current (0.01 m/s) with a greater concentration and elevated concentration gradient.

CONCLUDING REMARKS

The above exercise leads to the following general observations:

(1) Since field data available at the Alleppey site were very sparse in terms of temporal and spatial spread, model calibration and verification have severe limitations. Improvements in the calibration procedure and predictive ability of the model can only be brought about from a more comprehensive field data collection effort.

(2) As noted, current-induced boundary layer measurably influences wave-induced sediment resuspension. We therefore wish to stress the sensitivity of mud dynamics at the Alleppey mudbanks to the ambient current field, which at present is very poorly defined.

(3) The simulation method presented emphasizes the significance of local vertical transport mechanism in determining the structure and dynamics of suspended sediment profiles in the mudbank area.

(4) Under the present state-of-of-the-art, formulation of process equations for entrainment and deposition of fine sediments in any situation involves use of a number of empirical parameters that are flow- and sediment-related. Hence their appearance is unavoidable in the governing equations for fine sediment transport dealing with the application to a situation such as mudbanks. In spite of this limitation, it should be possible to obtain reasonably reliable site-specific predictions of suspended sediment variation, provided adequate field data are available for selecting representative values of the empirical parameters in the model.

In view of the importance of field data collection at Alleppey, the following general strategy is suggested. As a first step, a sediment budget should be established, both as a means to determine mud sources and sinks, and to quantify mud transport. For documenting spatial variability in sediment loads, and motion of bottom mud, it will be essential to set up dedicated tower assemblies for measuring waves, current velocities, suspended sediment concentration profiles and bottom sediment density profiles (MEHTA, 1991b). To that end the near-bottom region, where steep concentration gradients typically occur, must be sampled at close vertical spacing. The importance of this sampling in highlighted by the fact that the majority of suspended sediment transport characteristically occurs below the steep concentration gradient, so that quantification of the near-bottom sediment load is critical for establishing a regional sediment budget. Sub-bottom acoustic scanning is recommended for determining the extent of mud and its thickness (KIRBY *et al.*, 1994).

ACKNOWLEDGEMENT

Partial support for this work was received by the University of Florida from the U.S. Army Engineer Waterways Experiment Station contract DACW39-95-K-0022 through the Hydraulics Laboratory, with funding provided by the New

York District. Professor Ashish J. Mehta was the principal investigator of the study. The Chief of Engineers has given permission to publish this paper.

LITERATURE CITED

CERVANTES E.E.; MEHTA A.J., and LI Y., 1995. A laboratory-based examination of "episodic" resuspension of fine-grained sediments by waves and current. *Proceedings of the Fourth International Conference on Coastal and Port Engineering in Developing Countries*, Brazilian Water Resources Association (ABRH), Rio de Janeiro, 1–13.

DE WITT P.J., 1995. Liquefaction of Cohesive Sediments Caused by Waves. Ph. D. Thesis, Delft Technical University, Delft, The Netherlands, 209p.

DYER K.R., 1986. *Coastal and Estuarine Sediment Dynamics*. New York: Wiley, 357p.

FAAS R.W., 1995. Mudbanks of the southwest coast of India. III: Role of non-Newtonian flow properties in the generation and maintenance of mudbanks. *Journal of Coastal Research*, 11(3), 911–917.

HWANG K.-N., 1989. Erodibility of fine sediment in wave-dominated environments. *Report UFL/COEL-89/017*, Coastal and Oceanographic Engineering Department, University of Florida, Gainesville, 158p.

HWANG P.A. and WANG H., 1982. Wave kinematics and sediment suspension at wave breaking point. *Technical Report* No. 13, Department of Civil Engineering, University of Delaware, Newark, DE, 173p.

JIANG F., 1993. Bottom Mud Transport Due to Water Waves. Ph. D. Thesis, University of Florida, Gainesville, Florida, 222p.

JIANG F. and MEHTA A.J., 1992. Some observations on fluid mud response to water waves. *In:* D. PRANDLE (ed.), *Dynamics and Exchanges in Estuaries and the Coastal Zone*. Washington, DC: American Geophysical Union, pp. 351–376.

JIANG F. and MEHTA A.J., 1995. Mudbanks of the southwest coast of India. IV: Mud viscoelastic properties. *Journal of Coastal Research*, 11(3), 918–926.

JIANG F. and MEHTA A.J., 1996. Mudbanks of the southwest coast of India. V: Wave attenuation. *Journal of Coastal Research*, 12(4), (in press).

KEMP G.P. and WELLS J.T., 1987. Observations of shallow-water waves over a fluid mud bottom: implications to sediment transport. *Proceedings of Coastal Sediments'87* (ASCE), New York, pp. 363–377.

KIRBY R.; HOBBS C.H., and MEHTA A.J., 1994. Shallow stratigraphy of Lake Okeechobee, Florida: a preliminary reconnaissance. *Journal of Coastal Research*, 10(2), 339–350.

KRANENBURG C., 1994. An entrainment model for fluid mud. *Report 93-10*, Faculty of Civil Engineering, Delft University of Technology, Delft, The Netherlands, 23p.

KRONE R.B., 1993. Sedimentation revisited. *In:* A.J. Mehta, (ed.), *Nearshore and Estuarine Cohesive Sediment Transport*, Washington, DC: American Geophysical Union, pp. 108–125.

LI Y., 1996. Sediment-associated constituent release at the mud-water interface due to monochromatic waves. Ph.D. Thesis, University of Florida, Gainesville, Florida, 344p.

MAA P.-Y., 1986. Erosion of soft muds by waves. *Report UFL/COEL-TR/059*, Coastal and Oceanographic Engineering Department, University of Florida, Gainesville, FL, 296p.

MAA P.-Y. and MEHTA A.J., 1987. Mud erosion by waves: A laboratory study. *Continental Shelf Research*, 7(11/12), 1269–1284.

MADSEN O.S., 1991. Mechanics of cohesionless sediment transport in coastal waters. *Proceedings of Coastal Sediments'91* (ASCE, New York), pp. 15–27.

MATHEW J., 1992. Wave–mud interaction in mudbanks. Ph.D. Dissertation, Cochin University of Science and Technology, Cochin, Kerala, India, 139p.

MATHEW J.; BABA M., and KURIAN N.P., 1995. Mudbanks of the southwest coast of India. I: Wave characteristics. *Journal of Coastal Research*, 11(1), 168–178.

MATHEW J. and BABA M., 1995. Mudbanks of the southwest coast of India. II: Wave-mud interactions. *Journal of Coastal Research*, 11(1), 179–187.

MEHTA A.J., 1988. Laboratory studies on cohesive sediment deposition and erosion. *In:* J. DRONKERS and W. VAN LEUSSEN (eds.), *Physical Processes in Estuaries*, Berlin: Springer-Verlag, pp. 427–445.

MEHTA A.J., 1994. Hydraulic behavior of fine sediment. *In*: M.B. ABBOTT and W.A. PRICE (eds.), *Coastal, Estuarial and Harbour Engineer's Reference Book*, London: Chapman & Hall, pp. 577–584.

MEHTA A.J., 1991a. Review notes on cohesive sediment erosion. *Proceedings of Coastal Sediments'91*, (ASCE, New York), pp. 40–53.

MEHTA A.J., 1991b. Strategy for fine sediment regime investigation: Lake Okeechobee, Florida. *Proceedings of the Third Conference on Coastal and Port Engineering in Developing Countries* (Mombasa, Kenya), pp. 903–917.

MEHTA A.J.; PARTHENIADES E.; DIXIT J.G., and MCANALLY W.H., 1982. Properties of deposited kaolinite in a long flume. *Proceedings of the Conference on Applying Research to Hydraulic Practice* (ASCE, New York), pp. 594–603.

MEHTA A.J. and SRINIVAS R., 1993. Observations on the entrainment of fluid mud by shear flow. *In*: A.J. MEHTA (ed.), Nearshore *and Estuarine Cohesive Sediment Transport*, Washington, DC: American Geophysical Union, pp. 224–246.

MEHTA A.J.; WILLIAMS D.J.A.; WILLIAMS P.R., and FENG J., 1995. Tracking dynamic changes in mud bed due to waves. *Journal of Hydraulic Engineering*, 121(5), 504–506.

MUNK W.H. and ANDERSON E.R., 1948. Notes on a theory of the thermocline. *Journal of Marine Research*, 1, 276–295.

NAIR A.S.K., 1988. Mudbanks (chakara) of Kerala—A marine environment to be protected. *Proceedings of the National Seminar on Environmental Issues*, University of Kerala Golden Jubilee Seminar, Thiruvananthapuram, Kerala, India, 76–93.

PARCHURE T.M. and MEHTA A.J., 1985. Erosion of soft cohesive sediment deposits. *Journal of Hydraulic Engineering*, 111(10), 1308–1326.

ROSS M.A., 1988. Vertical Structure of Estuarine Fine Sediment Suspensions. Ph. D. Thesis, University of Florida, Gainesville, Florida, 206p.

SANFORD L.P., 1994. Wave-forced resuspension of upper Chesapeake Bay muds. Estuaries, 17(1B), 148–165.

SANFORD L.P. and HALKA J.P., 1993. Assessing the paradigm of mutually exclusive erosion and deposition of mud, with examples from upper Chesapeake Bay. *Marine Geology*, 114, 37–57.

SCARLATOS P.D. and MEHTA A.J., 1993. Instability and entrainment mechanisms at the stratified fluid mud-water interface. *In*: A.J. MEHTA (ed.), *Nearshore and Estuarine Cohesive Sediment Transport*, Washington, DC: American Geophysical Union, pp. 205–223.

TAKI K., 1990. Hydraulic Study on the Rate of Resuspension of Mud Due to Free Surface Water Flow. Ph. D. Thesis, Chuo University, Tokyo, 180p, (In Japanese).

THIMAKORN P., 1980. An experiment on clay resuspension under water waves. *Proceedings of the 17th Coastal Engineering Conference*, (ASCE, New York) Vol. 3, pp. 2894–2906.

THIMAKORN P., 1984. Resuspension of clays under waves. In: B. DENNESS (ed.), *Seabed Mechanics*. London: Graham & Trotman, pp. 191–196.

VAN LEUSSEN W., 1994. Estuarine Macroflocs and Their Role in Fine-Grained Sediment Transport. Ph. D. Thesis, University of Utrecht, Utrecht, The Netherlands, 488p.

WINTERWERP, J.C.; CORNELISSE J.M., and KUIJPER C., 1993. A laboratory study on the behavior of mud from the Western Scheldt under tidal conditions. *In*: A.J. MEHTA (ed.), *Nearshore and Estuarine Cohesive Sediment Transport*. Washington, DC: American Geophysical Union, 295–313.

WOLANSKI E.; GIBBS R.J.; MAZDA Y.; MEHTA A., and KING B., 1992. The role of2turbulence in the settling of mud flocs. *Journal of Coastal Research*, 8(1), 35–46.